

Fluctuations in $YBa_2Cu_3O_{6.5}$ single crystal: an evidence for $2D \rightarrow 3D$ crossover

B. Rosenstein,* B. Ya. Shapiro,† R. Prozorov,‡ A. Shaulov, and Y. Yeshurun

*Institute for Superconductivity, Department of Physics,
Bar-Ilan University, 52900 Ramat-Gan, Israel*

(Dated: November 20, 2018)

Magnetization measurements as a function of temperature are reported for $YBa_2Cu_3O_{6.5}$ crystal ($T_c = 45.2$ K) for fields between 0.2 to 3.5 Tesla. All isochamps for $H > 1$ Tesla intersect at $T_{2D}^* \simeq 42.8$ K, implying fluctuations contribution to the magnetization. These curves collapse into a single curve when magnetization and temperature are scaled according to the predicted "2D scaling" in the fluctuation regime. Surprisingly, the low field curves also intersect, at $T_{3D}^* \simeq 43.4$ K, and they obey a 3D scaling. We provide a theoretical picture of the magnetization in the fluctuation regime based on the Lawrence-Doniach model. Within this model we calculate the field and temperature dependence of the magnetization. The two intersection points and the $2D \rightarrow 3D$ crossover are consistent with the experimental observation.

INTRODUCTION

High-temperature superconductors (HTS) are characterized by a wide temperature range in which fluctuations are important [1, 2]. This range is proportional to the Ginzburg parameter Gi , which is very sensitive both to the dimensionality D of the system and to the superconducting coherence length ξ . Thus, strong fluctuations, usually negligible in conventional superconductors, become extremely important due to the small ξ and quasi two-dimensional structure.

A useful tool in the analysis of the nature of critical fluctuation is the dimensionality dependent scaling of the magnetization M versus temperature T for various DC magnetic fields H [3] in part of the phase diagram that is "not very far" from $H_{c2}(T)$ [4]. The scaled magnetization $m = M / (HT)^{(D-1)/D}$ is plotted versus the scaled temperature $a_T = (T - T_c(H)) / (HT)^{(D-1)/D}$ and all isochamps are predicted to collapse onto a single curve according to a dimensionality of the system [5, 6]. Once such a scaling is found, the "fluctuation" dimensionality D can be determined. In 2D systems the relative contribution of the fluctuations to the magnetization is much larger than in 3D systems. Experimentally, the scaling approach has been widely employed to study the highly anisotropic, quasi 2D, $Bi - Sr - Ca - Cu - O$ (2223) [6] and (2212) [5, 7, 8, 9], where two-dimensional scaling was shown to work very well. The same 2D scaling seems to work also for $Tl - Ca - Ba - Cu - O$ (2223) [10, 11], (2201) [5, 12], (2212) [5, 11] and (2223) [11], and for $Hg - Ba - Ca - Cu - O$ (1223)[13], (1201) [10], and (1212) [14].

The contribution of fluctuations to the magnetization is also borne out in the experiment as a crossing point of all isochamps at a temperature T^* [3, 7, 8]. At this temperature M is independent of H for a large range of fields. This feature was previously observed experimentally in 2D systems where 2D scaling was expected [5, 6, 9, 10, 11, 12, 13, 14]. Theoretically there is evidence that in both 2D and 3D the intersection is not perfect, the intersection points however are very close to each other, especially in 2D [15]. Though most HTS are either 2D or 3D materials, there is, in principle, a possibility that both 3D and 2D behaviors would be measured at the same sample, depending on magnetic field and temperature. Such 2D to 3D crossover in vortex fluctuations is expected for highly anisotropic superconductors, at high temperatures, simply because the coherence length ξ diverges as T approaches the transition temperature T_c . An evidence for a temperature induced crossover was found in magnetization measurements in $YBa_2Cu_3O_7$ [16]. Another possible experimental approach to study the $2D \rightarrow 3D$ crossover may be based on the expected change in the anisotropy caused by changing the oxygen content in $Y - Ba - Cu - O$. In this system, the anisotropy increases with the decrease in the oxygen content. Indeed, a 3D scaling was observed in a fully oxygenated $YBa_2Cu_3O_7$ single crystal [17], but a 2D scaling was demonstrated [18] in $YBa_2Cu_3O_{6.6}$.

In the present work we establish, experimentally and theoretically, the existence of a 2D to 3D crossover in the nature of fluctuations in a high T_c superconductor. Specifically, in the oxygen deficient $YBa_2Cu_3O_{6.5}$ ($T_c \approx 45.15$ K) single crystal, at high fields (above 1 Tesla), the magnetization isochamps intersect at one temperature T_{2D}^* (Fig.1) and exhibit a 2D type of scaling. However, at the lower fields we find another, somewhat smeared, crossing point at T_{3D}^* (Fig.2), and the magnetization exhibits a 3D scaling. The presence of two intersection points, as well as 2D and 3D scaling of magnetization in different field regimes, are the new experimental points in this work. If one defines a field dependent "intersection point" as an intersection of two lines for close magnetic fields, one observes that as field is lowered, the intersection point first "sits" at (M_{2D}^*, T_{2D}^*) , than jumps quickly to (M_{3D}^*, T_{3D}^*) and nearly stops there. Preliminary discussions of these results were presented in Ref. [19]. In the current paper we provide a theoretical

picture of the fluctuation in different regimes of the field-temperature ($H - T$) plane showing a $2D \rightarrow 3D$ crossover in accordance with the experimental results. We calculate the magnetization of the Lawrence - Doniach model describing layered superconductors using the "bubble" diagram resummation analogous to that established earlier in the $2D$ and $3D$ limiting cases [20]. The results are compared in the $2D$ and $3D$ limits and also between these limits where scaling does not hold.

EXPERIMENT

Details of sample preparation are given in [21]. The magnetization of the $2.45 \times 3.85 \times 0.8 \text{ mm}^3$ $YBa_2Cu_3O_{6.5}$ single crystal was measured by a "Quantum Design" SQUID magnetometer. The high temperature part of the magnetization ($46 - 200 \text{ K}$) was fitted to a Curie law, $M = \chi H = (\chi_0 + C/T)H$, and extrapolated to temperatures below T_c . The extrapolated values of M were subtracted from the raw data measured below T_c . This procedure was repeated for each value of the applied magnetic field. In Fig. 1 we show the temperature dependence of the magnetization for various magnetic fields $H > 1 \text{ Tesla}$. All these curves intersect at $T = T_{2D}^* \simeq 42.8 \text{ K}$, indicating fluctuational contribution to the magnetization [3, 7, 8]. The subscript $2D$ is justified by the success of the $2D$ scaling procedure described in Fig. 3 where we plot $M/(HT)^{1/2}$ versus $(T - T_c(H))/(HT)^{1/2}$ for magnetization curves between 1 and 3 Tesla.

Low-field measurements ($H < 1 \text{ Tesla}$) are shown in Fig. 2. Another intersection point, at $T = T_{3D}^* \simeq 43.4 \text{ K}$, is found in this field range. This group of curves can be scaled by using the $3D$ scaling procedure. This is demonstrated in Fig. 4 where we plot $M/(HT)^{2/3}$ versus $(T - T_c(H))/(HT)^{2/3}$ for magnetization curves between 0.2 and 0.75 Tesla. These observations imply a $2D \rightarrow 3D$ crossover in the vortex fluctuation regime of our sample.

THEORY

In order to find domains of different fluctuation behavior in the $H - T$ phase diagram one has to calculate the fluctuational part of the magnetization M defined by the partition function Z :

$$M = -\frac{1}{4\pi} \frac{\partial F}{\partial H}; \quad F = -T \ln Z; \quad Z = \int D\psi D\psi^* \exp(-\mathcal{H}_{LD}/T) \quad (1)$$

where F is a free energy. In the general case of a layered superconductor with Josephson inter-layer coupling the Hamiltonian H_{LD} has the well known Lawrence-Doniach (LD) form [22]:

$$\mathcal{H}_{LD} = \sum_n N(\epsilon_F) \int d^2\mathbf{r} \left[\xi_{ab}^2 \left| \left(-i\nabla - \frac{2e}{\hbar c} \mathbf{A} \right) \psi_n \right|^2 + \frac{\gamma}{2} |\psi_n - \psi_{n+1}|^2 + (t-1) |\psi_n|^2 + \frac{\beta}{2} |\psi_n|^4 + \frac{1}{8\pi} (\nabla \times \mathbf{A})^2 \right]. \quad (2)$$

The magnetic field is assumed to be constant and oriented perpendicularly to the layers (xy) and its fluctuations neglected. We use the Landau gauge: $\mathbf{A} = (0, Hx, 0)$. In Eq.(2) $\psi_n(x, y)$ is the order parameter in the n -th layer, $N(\epsilon_F)$ is (the $2D$) density of states within the layer, ξ_{ab} is the in-plane coherence length, β - the Ginzburg-Landau (GL) coefficient, $\gamma = (\xi_c/d)^2$ is a dimensionless parameter describing the inter-layer coupling, where d is the inter-layer spacing and $t = T/T_c$. This Hamiltonian describes the strong in-plane superconducting fluctuations and their inter-layer interactions and can manifest both $3D$ and $2D$ behavior in limiting cases as shown below.

The nonlinear term $|\psi_n|^4$ in the Hamiltonian becomes very important in the temperature range $|1 - t| \sim Gi$ at the broad region near the transition line, preventing an exact solution of the Hamiltonian in this regime. We are able, however, to apply various approximations, as described below, and to show that free energy F can exhibit a $3D \rightarrow 2D$ crossover as temperature or field are changed. We then are able to approximate the intersection point of the magnetization curves in both $2D$ and $3D$ limits.

The magnetic moment of fluctuations described by the Hamiltonian (2) may be approximately found in three limiting cases: (i) The $3D$ XY model [23], (ii) the $3D$ lowest Landau levels (LLL) approximation, and (iii) the $2D$ LLL approximation [20]. Case (i) is not relevant for our experiments since it applies to too low magnetic fields. Cases (ii) and (iii) are studied here. In the region of strong fluctuations it is convenient to expand the order parameter in terms of the Landau levels eigenfunctions [24]

$$\psi_n^N(\mathbf{r}) = \sum_{k,q} \phi_{k,q}^N(\mathbf{r}) a_{k,q}^N \quad (3)$$

$$\phi_{k,q}^N(\mathbf{r}) = \frac{1}{\sqrt{L_x L_y}} \left(\frac{2eH}{\pi \hbar c 2^N N!} \right)^{1/4} H_N \left(x - \frac{q \hbar c}{2eH} \right) \exp \left[i q y + i k d N - \frac{eH}{\hbar c} \left(x - \frac{q \hbar c}{2eH} \right)^2 \right] \quad (4)$$

where N stands for Landau level number and summation index q bears in mind degeneration of the LLL state.

In the field and temperature ranges of the experiment one can rely on the LLL approximation [4]. Therefore, we retain in the Hamiltonian only terms with $N = 0$:

$$\mathcal{H}_{LD} = \sum_{q,k} |a_{k,q}|^2 [a_H + \gamma(1 - \cos kd)] + \frac{\beta}{2} P \quad (5)$$

where

$$a_H = \frac{2eH}{\hbar c} \xi_{ab}^2 + t - 1$$

is a dimensionless temperature parameter, and

$$P = \sum_{k_i q_i} I(k_1, k_2, k_3, k_4) a_{k_1, q_1}^* a_{k_2, q_2}^* a_{k_3, q_3} a_{k_4, q_4}.$$

Here

$$k_1 + k_2 = k_3 + k_4$$

$$q_1 + q_2 = q_3 + q_4$$

$$I(k_1, k_2, k_3, k_4) = \int d^2 \mathbf{r} \prod_{i=1,2,3,4} \phi_{k_i, q_i}(\mathbf{r}).$$

Since we are interested in vortex liquid phase we will use the renormalized high temperature expansion proposed for the $2D$ and $3D$ cases by Thouless and coworkers [20]. The first step is to perform a summation of all the "bubble" diagrams. This is equivalent to a kind of mean field approximation in which $|\psi_n|^4 - \langle |\psi_n|^2 \rangle \langle |\psi_n|^2 \rangle$. In this approximation the Hamiltonian (2) becomes

$$\mathcal{H}_{LD}^{MF} = \sum_{q,k} |a_{k,q}|^2 \left[a_H + \gamma(1 - \cos kd) + \frac{\beta}{2} \sum_{q,k} \frac{\langle |a_{k,q}|^2 \rangle}{L_x L_y} \right] \frac{N(\epsilon_F)}{d} \quad (6)$$

The dimensionless average

$$\Delta \equiv \frac{\beta}{2} \sum_{q,k} \frac{\langle |a_{k,q}|^2 \rangle}{L_x L_y}$$

can be found self-consistently by solving the gap equation:

$$\Delta = \frac{T d \beta}{2 L_x L_y N(\epsilon_F)} \sum_{q,k} \frac{1}{a_H + \gamma(1 - \cos kd) + \Delta} = \frac{2 T \beta e H}{N(\epsilon_F) \pi \hbar c} \frac{1}{\sqrt{(a_H + \gamma + \Delta)^2 - \gamma^2}} \quad (7)$$

The magnetization calculated from Eq.(1), using the mean field Hamiltonian (2), is

$$M = - \frac{e N(\epsilon_F) \xi_{ab}^2}{\pi \beta \hbar c d} \Delta. \quad (8)$$

For convenience, we convert the expression for Δ into a dimensionless form

$$\Delta = g \frac{bt}{\sqrt{(b+t+\Delta+\gamma-1)^2 - \gamma^2}}, \quad (9)$$

where

$$b = \frac{H}{H_{c2}(0)}; \quad g = \frac{2T_c \beta e H_{c2}(0)}{N(\epsilon_F) \pi \hbar c}.$$

The dimensionless coupling constant g is proportional to the $2D$ Ginzburg number.

We consider two limits for which the gap equation can be solved *analytically*. The first case refers to the domain of the $H - T$ phase diagram where

$$\gamma \ll \frac{1}{2} \left(\sqrt{(b+t-1)^2 + 4bt} + (b+t-1) \right) \quad (10)$$

namely, for the experiments at relatively high fields. In this case, a well known $2D$ result (see [4]) reads:

$$\begin{aligned} \Delta &= (\sqrt{bt}) f_{2D}(u); \quad u = \frac{b+t-1}{2\sqrt{bt}}, \\ f_{2D}(u) &= \sqrt{u^2 + 1} - u \end{aligned} \quad (11)$$

where

$$b+t-1 = \frac{T - T_c(H)}{T_c}$$

The magnetization in this limit demonstrates a well pronounced $2D$ scaling dependence

$$\frac{M}{\sqrt{HT}} \propto f_{2D} \left(\frac{T - T_c(H)}{\sqrt{HT}} \right) \quad (12)$$

The second case refers to the limit

$$\gamma \gg b+t-1 + \frac{2((b+t-1)^3)}{27}, \quad \text{and } V = \frac{4((b+t-1)^3 \gamma)}{27g^2(bt)^2} > \frac{1}{2} \quad (13)$$

namely for the experiments at relatively low fields. In this case,

$$\Delta = [(bt)^{2/3}] \left(\frac{g^2}{\gamma} \right)^{1/3} f_{3D}(V) \quad (14)$$

where

$$f_{3D}(V) = 2V^{1/3} \sin\left(\frac{\pi}{6} - \frac{\varphi}{3}\right) - \left(\frac{V}{2}\right)^{1/3}$$

and

$$\tan \varphi = \frac{\sqrt{2V-1}}{1-V}. \quad (15)$$

Apparently, the behavior of the magnetization in this case is caused by $3D$ fluctuations:

$$\frac{M}{(HT)^{2/3}} \propto f_{3D} \left(\frac{T - T_c(H)}{(HT)^{2/3}} \right) \quad (16)$$

In both limits one clearly finds a scaling behavior, manifested in Figures 3 and 4. For an intermediate magnetic field, however, scaling is not expected even though the LLL approximation is still valid. In this intermediate case the scale is provided by the inter-layer spacing d .

TABLE I: Parameters used for calculations of theoretical curves in Figs. 1 , 2, and 5.

Parameter	Value used
T_c	45.15 <i>K</i>
$\frac{dH_{c2}}{dT} _{T=T_c}$	4 <i>Tesla/K</i>
$\xi_{ab}(0)$	14 <i>Å</i>
$\frac{\beta}{N(\varepsilon_F)}$	$0.65 \frac{sec^2}{g}$
d	5 <i>Å</i>
β_{BCS}	$2.6 \times 10^{27} erg^{-2}$
$N(\varepsilon_F)$	$4 \times 10^{27} \frac{1}{erg cm^2}$
$\xi_c(0)$	0.5 <i>Å</i>
$\frac{m_c}{m_{nb}} = \left(\frac{\xi_{ab}}{\xi_c}\right)^2$	850

FITS AND DISCUSSION

The solid lines in Figures 1, 2, and 5 are the theoretical magnetization *vs.* temperature curves derived from Eq. (11) for the 2*D*-behavior (Fig. 1), from Eq. (15) for the 3*D* behavior (Fig. 2), and from Eq. (8) for the intermediate case (Fig. 5). Also, as implied by Eqs. (12) and (16), in both the 2*D* and the 3*D* cases the magnetization data is expected to scale. Both of these formulas obey the respective scaling conditions as demonstrated by the solid lines in Figures 3 and 4 derived from Eqs. (11) and (14), respectively. All the "2*D*" experimental curves intersect at about $T_{2D}^* / T_c \simeq 0.948$ and the 3*D* curves approximately intersect at somewhat higher temperature $T_{3D}^* / T_c \simeq 0.960$. Table I summarizes the superconducting parameters used in our analysis to fit the experimental data.

The parameters were derived in the following way: The transition temperature T_c was derived directly from the magnetization data. The slope $\frac{dH_{c2}}{dT}|_{T=T_c} = 4 \text{ Tesla/K}$, yielding $H_{c2}(0) = 180 \text{ Tesla}$, gave the best fit to the experimental data for both intersection points. Here we use the notation $H_{c2}(0)$ to denote $T_c \frac{dH_{c2}}{dT}|_{T=T_c}$ rather than unknown upper critical field at zero temperature. The latter is unknown and sometimes is estimated as 70% of this quantity as in BCS theory inapplicable to the present case. The coherence length was defined by $\xi_{ab}(0) = \sqrt{\Phi_0/2\pi H_{c2}(0)}$. It should be noted that here $\frac{dH_{c2}}{dT}|_{T=T_c}$ is the mean field theoretical parameter rather than experimentally measured; direct measurement of this value is expected to yield a smaller value due to contribution of fluctuations [25]. The value of the dimensionless coupling constant $g = 0.07$, the *interlayer-coupling* parameter $\gamma = 0.008$, and the magnetization $M_{2D}^* = -2.5 \times 10^{-4} \text{ emu}$ at the 2*D* intersection point, determine the ratio $\frac{\beta}{N(\varepsilon_F)}$, d , and $\xi_c(0)$. Assuming the validity of the BCS expression for $\beta = \frac{7\zeta(3)}{8\pi^2 T_c^2}$ one gets a rough estimate of the density of states. Now we discuss the applicability of the 2*D* and 3*D* limits to describe the regions around the crossing points as was done on Fig.1 and 2. The inequality 10 for $t = T^*/T_c = .95$, so that $1 - t \gg b = .001$ simplify into $b \gg \gamma^*(1 - t) = .2 \text{ Tesla}/H_{c2}(0)$. Similarly the condition of applicability of the 3*D* limit (see Eq. (13)) can be simplified into $b \ll 1 - t - \gamma = 5 \text{ Tesla}/H_{c2}(0)$. The use of the 2*D* limit in Fig.1 is therefore justified for $B = 1.5 \text{ Tesla}$ or larger, while for $B \leq .75 \text{ Tesla}$ the use of the 3*D* limit in Fig.2 is justified.

To conclude, a crossover between 2*D* and 3*D* behavior in the magnetization of $YBa_2Cu_3O_{6.5}$ was observed and described theoretically by employing the Lawrence - Doniach model in lowest Landau level approximation in the fluctuation regime. The model yields analytical expressions for *two* intersection points of the magnetization curves, as observed experimentally. One intersection point, for magnetization curves at relatively high fields, is a result of fluctuations in the 2*D* regime. The second intersection point, for relatively low fields, is a result of fluctuations in the 3*D* regime. The model also predicts scaling of the magnetization data in the 2*D* and the 3*D* regimes, as observed experimentally.

This work was supported by The Israel Science Foundation - Center of Excellence Program, and by the Heinrich Hertz Minerva Center for High Temperature Superconductivity. Y.Y. acknowledges support from the U.S.-Israel Binational Science Foundation. We thank A. Erb and H. Wuhl for providing the YBCO sample. B. S. and A.S. acknowledge support from the Israel Academy of Science and Humanities. B.R. is very grateful to the Physics Department at Bar Ilan University for the warm hospitality.

* Permanent address: Nat. Center for Theoretical Sciences and Electronic Physics Department, Nat. Chiao Tung University, Hsinchu, Taiwan, R.O.C.

† Corresponding author

‡ Present address: Loomis Laboratory of Physics, University of Illinois at Urbana-Champaign, IL 61801, U.S.A.

- [1] A. Wahl, V. Hardy, F. Warmont, A. Maignan, M. P. Delamare, and Ch. Simon, Phys. Rev. B **55**, 3929 (1997).
- [2] A. Junod, J.-Y. Genuod, G. Triscone, and T. Schneider, Physica C **294**, 115 (1998).
- [3] Z. Tešanović, L. Xing, L. Bulaevskii, Q. Li, and M. Suenaga, Phys. Rev. Lett. **69**, 3563 (1992).
- [4] I. D. Lawrie, Phys. Rev. **B50**, 9456 (1994); D. Li and B. Rosenstein, Phys. Rev. **B60** 9704, 10460 (1999).
- [5] G. Triscone, A. F. Khoder, C. Opagiste, J. Y. Genoud, T. Graf, E. Junod, T. Tsukamoto, M. Couach, A. Junod, J. Muller, Physica C **224**, 263 (1994).
- [6] Q. Li, M. Suenaga, L. N. Bulaevskii, T. Hikata, and K. Sato, Phys. Rev. B **48**, 13865 (1993); Q. Li, M. Suenaga, J. Gohng, D. K. Finnemore, T. Hikata, and K. Sato, Phys. Rev. B **46**, 3195 (1992).
- [7] V. G. Kogan, M. Ledvij, A. Y. Simonov, J. H. Cho, and D. C. Johnston, Phys. Rev. Lett. **70**, 1870 (1993); P. H. Kes, C. J. van der Beek, M. P. Maley, M. E. McHenry, D. A. Huse, M. J. V. Menken, and A. A. Menovsky, Phys. Rev. Lett. **67**, 2383 (1991).
- [8] L. N. Bulaevskii, M. Ledvij, and V. G. Kogan, Phys. Rev. Lett. **68**, 3773 (1992).
- [9] K. Kadowaki, Physica C **185 - 189**, 2249 (1991); R. Jin, H. R. Ott, and A. Schilling, Physica C **235**, 1923 (1994); R. Jin, H. R. Ott, and A. Schilling, Physica C **235**, 1923 (1994).
- [10] J. R. Thompson, D. K. Christen, and J. G. Ossandon, Physica B **194 - 196**, 1557 (1994).
- [11] A. Wahl, A. Maignan, C. Martin, V. Hardy, J. Provost, and C. Simon, Phys. Rev. B **51**, 9123 (1995).
- [12] F. Zuo, D. Vacaru, H. M. Duan, and A. M. Hermann, Phys. Rev. B **47**, 8327(1993).
- [13] M.-K. Bae, M. S. Choi, M.-O. Mun, S. Lee, S.-I. Lee, W. C. Lee, Physica C **228**, 195 (1994).
- [14] Z. J. Huang, Y. Y. Xue, R. L. Meng, X. D. Qui, Z. D. Hao, C. W. Chu, Physica C **228**, 211 (1994).
- [15] R. Sasik and D. Straud, Phys. Rev. Lett. **75** 2582 (1995).
- [16] C. Baraduc, E. Janod, C. Ayache, and J. Y. Henry, Physica C **235**, 1555 (1994). Note that in this work the system is claimed to exhibit *2D* fluctuations *above* T_c with a subsequent transition to the *3D* state when temperature decreases.
- [17] S. Salem-Sugui and E. Z. Dasilva, Physica C **235**, 1919 (1994).
- [18] V. Gomis, I. Catalán, B. Martínez, A. Gou, X. Obradors, and J. Fontchuberta, Physica C **235–240**, 2623 (1994).
- [19] A. Poddar, R. Prozorov, Y. Wolfus, M. Ghinovker, B.Ya. Shapiro, A. Shaulov, Y. Yeshurun, Physica C **282-287**, 1299 (1997)
- [20] G. J. Ruggieri and D. J. Thouless, J. Phys. F **6**, 2063 (1976); S. Hikami, A. Fujita, and A. I. Larkin, Phys. Rev. B **44**, 10400 (1991); A. E. Koshelev, Phys. Rev. B, **50**, 506 (1994).
- [21] A. Erb, T. Biernath, G. Muller-Vogt, J. Cryst. Growth **132**, 389 (1993).
- [22] W. E. Lawrence and S. Doniach, *Proc. Twelfth Int. Conf. on Low Temperature Physics, Kyoto, 1970*, ed. by E. Kanda (Keigaku, Tokyo, 1971) p.361.
- [23] G. P. Mikitik, Sov. Phys. JETP **74**, 558 (1992). [*Zh. Eksp. Teor. Fiz.* **101**, 1042 (1992)].
- [24] R. Ikeda, T. Ohmi, and T. Tsuneto, J. Phys. Soc. Jpn. **58**, 1377 (1989); **59**, 1397 (1990).
- [25] B. Ya. Shapiro, JETP Lett., **46**, 569 (1987).

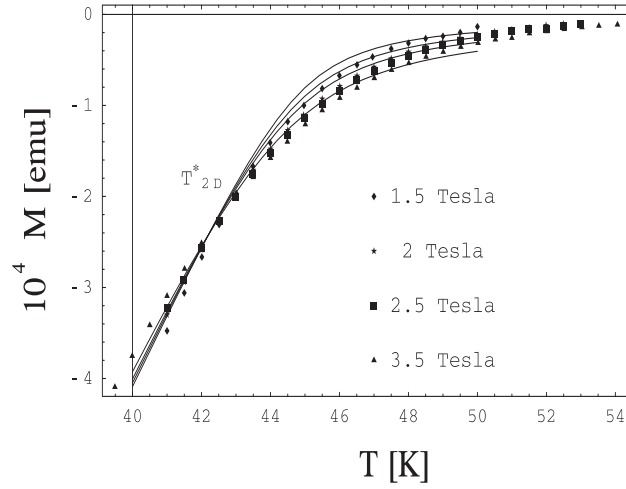


FIG. 1: Magnetic moment versus temperature in the high-field region ($1.5 - 3$ Tesla). The solid lines are fits to Eqs. (8) and (11) obeying the $2D$ scaling with the parameters listed in Table I.

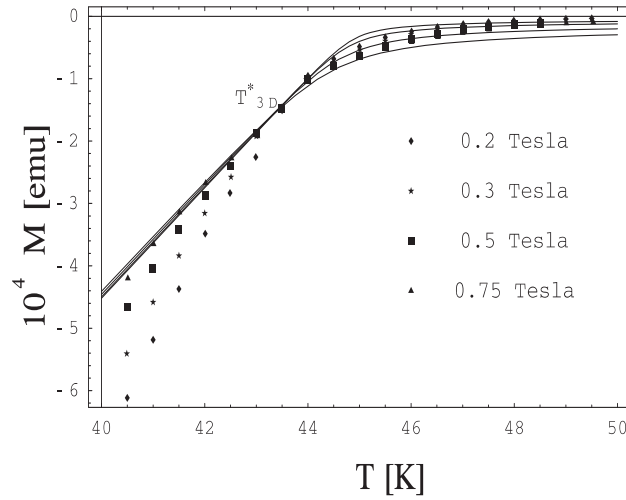


FIG. 2: Magnetic moment versus temperatures in the low-field region ($0.2 - 0.75$ Tesla). The solid lines are fits to Eqs. (8) and (15) obeying the $3D$ scaling with the parameters listed in Table I.

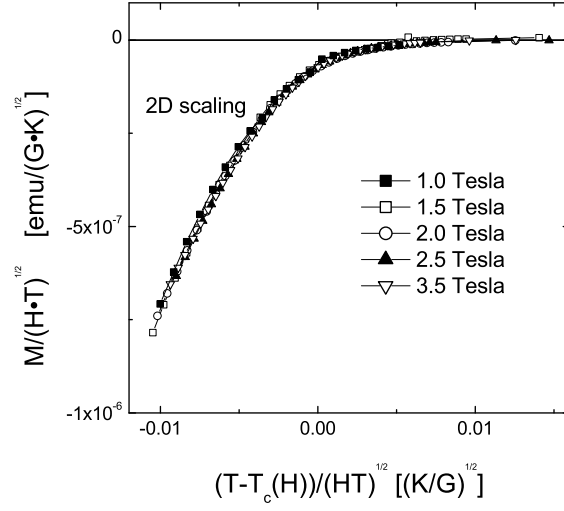


FIG. 3: Two-dimensional scaling of the high-field data. The solid line is a fit to Eq. ((12)).

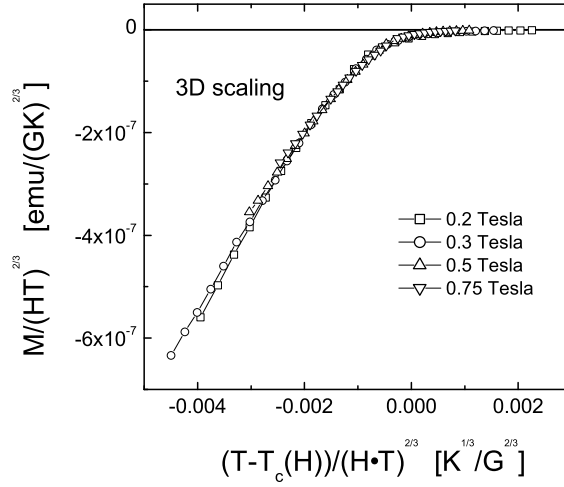


FIG. 4: Three-dimensional scaling of the low-field data. The solid line is a fit to Eq. (16).

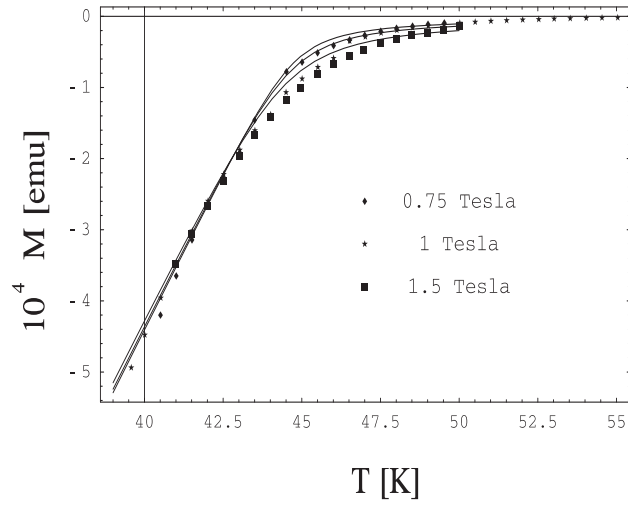


FIG. 5: Magnetic moment versus temperature for various magnetic fields around 1 *Tesla*. This field range represents an intermediate regime where $M(T)$ does not obey neither $3D$ nor $2D$ scaling; It is still described, however, in the framework of the Lawrence - Doniah model, Eqs. (8) and (9), as described by the solid lines.